HHS Public Access

Author manuscript

Ocul Surf. Author manuscript; available in PMC 2020 April 01.

Published in final edited form as:

Ocul Surf. 2019 April ; 17(2): 318–326. doi:10.1016/j.jtos.2018.12.006.

Clinical Signs of Meibomian Gland Dysfunction (MGD) are Associated with Changes in Meibum Sphingolipid Composition

Vikram Paranjpe, BS[1,2], **Jeremy Tan, MD**[4], **Jason Nguyen, MD**[5], **John Lee, BS**[1,2], **Jeremy Allegood, PhD**[6], **Anat Galor, MD, MSPH**[1,2,*], and **Nawajes Mandal, PhD**[3,*]

[1]Miami Veterans Administration Medical Center, 1201 NW 16th St, Miami, FL 33125

[2]Bascom Palmer Eye Institute, University of Miami, 900 NW 17th Street, Miami, FL 33136

[3]Departments of Ophthalmology, Anatomy and Neurobiology, University of Tennessee Health Sciences Center, Hamilton Eye Institute, 930 Madison Avenue, Memphis, TN 38163

[4]Ophthalmic Surgeons and Consultants of Ohio, Ohio State University, Columbus, OH 43203

[5]West Virginia University Eye, Morgantown, WV 26506

[6]Lipidomics Core, Department of Biochemistry and Molecular Biology, Virginia Commonwealth University School of Medicine, Richmond, VA 23249

Abstract

Purpose: Sphingolipids (SPL) play roles in cell signaling, inflammation, and apoptosis. Changes in SPL composition have been reported in individuals with MGD, but associations between clinical signs of MGD and compositional changes in meibum SPLs have not been examined.

Methods: Forty-three individuals underwent a tear film assessment. Groups were split into those with good or poor quality meibum. Meibum was collected then analyzed with liquid chromatography-mass spectroscopy to quantify SPL classes. Relative composition of SPL and major classes, Ceramide (Cer), Hexosyl-Ceramide (Hex-Cer), Sphingomyelin (SM), Sphingosine (Sph) and Sphingosine 1-phosphate (S1P) was calculated via mole percent.

Results: 22 and 21 individuals were characterized with good and poor quality meibum, respectively. Individuals with poor quality were older (60 ± 8 vs 51 ± 16 years) and more likely to be male (90% vs 64%). Relative composition analysis revealed that individuals with poor meibum

[*]**Corresponding Authors:** Nawajes Mandal, PhD, 930 Madison Avenue, Suite 718, Memphis, TN 38163; nmandal@uthsc.edu, Anat Galor, MD, MSPH, 900 NW 17th Street, Miami, FL 33136; agalor@med.miami.edu.

Declaration of interest: The authors report no conflicts of interest. The authors alone are responsible for the content and writing of the paper.

Role of sponsors: The above sponsors provided financial support to cover the researchers time but were not involved in the design and conduct of the study; collection, management, analysis, and interpretation of the data; preparation, review, or approval of the manuscript; or decision to submit the manuscript for publication. We would like to note that the contents of this study do not represent the views of the Department of Veterans Affairs or the United States Government.

Access to data: Anat Galor and Nawajes Mandal had full access to all the data in the study and take responsibility for the integrity of the data and the accuracy of the data analysis.

quality had SPL composed of less Cer (33.36% vs 49.49%, p<0.01), Hex-Cer (4.88% vs 9.15%, p<0.01), and S1P (0.16% vs 0.31%, p=0.05), and more SM (58.67% vs 38.18%, p<0.01) and Sph (2.92% vs 2.87%, p=0.97) compared to individuals with good quality meibum. Assessment of the ratio of Cer (pro-apoptotic) to S1P (pro-survival) showed that individuals with poor meibum quality had a relative increase in Cer (495.23 vs 282.69, p=0.07).

Conclusion: Meibum quality, a clinically graded marker of MGD, is associated with compositional changes in meibum sphingolipids. Further investigation of the structural and bioactive roles of sphingolipids in MGD may provide future targets for therapy.

Keywords

ceramide; sphingomyelin; dry eye; inflammation; meibomian gland dysfunction; sphingolipid; sphingosine 1-phosphate; tear film

Introduction

Dry eye (DE) is a multifactorial process manifesting with a variety of symptoms and signs caused by tear film modification in any of the three major tear constituents (mucin, aqueous, and lipid) and potential ocular surface damage and inflammation.[1,2] The prevalence of DE varies based on disease definition, geographic location, and among races, but the International Dry Eye Workshop estimated the overall prevalence to be between 5-30% in patients 50 years of age or older.[3] DE is classified into two subgroups; aqueous deficiency dry eye (ADDE) and evaporative dry eye (EDE), with EDE found to be the more prevalent type of DE in both clinic and population based studies.[3] ADDE is caused by inflammation of the lacrimal gland leading to decreased tear production, whereas EDE is related to disruption of the tear film lipid layer (TFLL) leading to evaporation of tears.[4]

Meibomian glands (MG), which are modified holocrine glands, secrete meibomian lipids or meibum, that then spreads across the ocular surface to form the TFLL.[4] EDE is often driven by meibomian gland dysfunction (MGD), most commonly obstructive MGD.[5-7] While the exact mechanisms behind obstructive MGD have not been fully elucidated, the central theme involves hyperkeratinization of the MG ductal epithelium.[8] Another theory posits that age-related MG atrophy is related to altered expression of the nuclear receptor, peroxisome proliferator-activated receptor gamma (PPARγ), as well as by the depletion of meibocyte stem cells with aging or other environmental stress.[9] PPARγ, which is thought to be a master regulator of meibocyte differentiation and function, was also found to regulate meibocyte lipid synthesis, suggesting that age-related MG atrophy and decreased lipid synthesis occur through a PPARγ-mediated pathway, in the absence of gland hyperkeratinization or obstruction.[9,10]

Regardless of the underlying mechanisms leading to disruption of MG function, clinically, patients with MGD are noted to have alterations in the quality and quantity of meibum, leading to tear film instability and clinical symptoms including dryness and irritation.[5,11-13] Meibum is composed of synthesized lipids (wax and sterol esters, diglycerides, triglycerides, hydrocarbons, and trace amounts of monoglycerides and fatty alcohols), membrane derived lipids (cerebrosides, phospholipids including phosphatidylcholine and sphingomyelin, and

trace amounts of ceramides) and bacterial degradation products (free-fatty acids).[6] Non-polar lipids (wax and sterol esters) comprise the largest portion of meibum (77%) and act as a lubricant and barrier to water. Polar lipids (phospholipids derived from the plasma membranes of acinar and ductal epithelial cells) constitute a lower percent (8%) of meibum and act as surfactants to help spread the TFLL across the ocular surface and also serve as structural supports for the non-polar lipids.[6]

Compositional changes in meibum, notably, an increase in polar lipids, have been noted in several ocular surface diseases including MGD.[6,11,14,15] Sphingolipids (SPL), which have been reported to comprise 30% of the polar lipids in meibum, are ubiquitous membrane lipids found in almost all cell types.[12] Prior studies[16-19] have focused on the structural role of polar lipids. McCulley and Shine[16] and Greiner et al[17] concluded that polar meibum lipids sit between the aqueous-mucin phase and non-polar meibum lipids, and provide crucial structural support to the non-polar lipids. *In vitro* studies have demonstrated that increasing meibum concentration of ceramide (Cer), a key SPL metabolite, led to an increased meibum melting temperature, increase in its rigidity at physiologic temperatures, and destabilization of the TFLL, thus further supporting its important structural role.[15,18] Beyond their structural role, SPL derivatives are bioactive and regulate important cellular functions such as apoptosis, proliferation, cell migration, and inflammation,[20-22] processes that are likely relevant to MGD as well. In fact, changes in SPL bioactivity are thought to underlie eye diseases such as optic neuritis associated with multiple sclerosis, uveitis, autoimmune conjunctivitis, age-related macular degeneration, retinitis pigmentosa, and diabetic retinopathy.[23] As such, compositional changes in meibum SPL likely affect both the structural and bioactive roles of SPL, and contribute to the clinical manifestations of MGD. Based on the above, we hypothesized that clinically graded markers of MGD associate with compositional changes in meibum SPL. In this study, we analyzed SPL composition in the meibum of individuals with and without clinical markers of MGD, focusing specifically on the major SPL species: ceramide (Cer), hexosyl ceramide (Hex-Cer), sphingosine 1-phosphate, (S1P), sphingomyelin (SM), and sphingosine (Sph).

METHODS

Study Population:

Miami Veterans Administration Medical Center (VAMC) and University of Oklahoma Health Sciences Center Institutional Review Board (IRB) approval allowed the prospective evaluation of patients. Informed consent was obtained from all patients, and the study was adherent with the principles of the Declaration of Helsinki. Patients with a wide variety of DE signs (none to severe) and no overt eyelid or corneal abnormalities were prospectively recruited from the Miami VAMC between October 2013 and August 2016. Patients were excluded if they wore contact lenses, had undergone refractive surgery, used ocular medications other than artificial tears, had active corneal infection or inflammation, had cataract surgery within the last 6 months, or any prior glaucoma or retinal surgery. Patients with human immunodeficiency virus, sarcoidosis, graft-versus-host disease, or a collagen vascular disease were also excluded.

Data Collected:

Demographics, past medical history and medication information were collected by self-report and verified by medical records.

Ocular surface evaluation:

All individuals underwent a standardized tear film assessment of both eyes including measurement of (1) tear osmolarity (TearLAB, San Diego, CA), (2) tear breakup time (TBUT), evaluated after 5μl of fluorescein was placed on the superior conjunctivae, (3) corneal staining with fluorescein using the National Eye Institute scale[2], (4) Schirmer's strips with anesthesia, and (5) meibomian gland (MG) assessment including characterization of meibum quality, inferior meibomian gland plugging (MG plugging), and meibomian gland dropout (MG atrophy). We graded MG plugging from 0 to 3, defined as: 0, none; 1, less than 1/3 lid involvement; 2, between 1/3 and 2/3 lid involvement; 3, greater than 2/3 lid involvement.[24,25] MG atrophy was assessed by the contact meibography technique using retroillumination and was quantified using a five-point scale (0, area of loss 0%; 1, area of loss <25%; 2, area of loss 25%-50%; 3, area of loss 51-75%; 4, area of loss >75%).[26] The quality of forcefully expressed meibum was graded on a scale of 0 to 4 (0, clear; 1, cloudy; 2, granular; 3, toothpaste; 4, no meibum extracted).[27]

Classification of MGD:

We characterized individuals as MGD or control for each analysis separately and used the score of the worse eye for each clinical marker (meibum quality, inferior MG plugging, or MG atrophy). Our primary predictor variable was clinically graded meibum quality. Individuals were first divided into two clinical groups, control, or those with good meibum quality (grade 0 or 1) and MGD, or those with poor meibum quality (grade, 2, 3, or 4). We then re-classified individuals using our other predictor variables including clinically graded inferior MG plugging scores and MG atrophy (meiboscale scores) independent of meibum quality. Individuals with MG plugging scores of 0 or 1 were defined as the control group and those with MG plugging scores of 2 or 3 were defined as the MGD group. Individuals with less than or equal to 25% MG atrophy (meiboscale score 0-1) were defined as the control group and those with greater than 25% MG atrophy (meiboscale score 2-4) were defined as the MGD group.

Sample collection:

A drop of proparacaine was placed on the ocular surface and on two cotton tip applicators. One applicator was placed behind and one in front of the interior tarsal plate and pressure was applied to forcefully express meibum from the inferior orifices. We placed the two cotton applicators centrally and applied pressure while moving the tips back and forth. On average, we tried to express meibum from at least five glands from each eye and collect all expressed meibum. The expressed meibum was collected by swiping the cotton tip applicator across the inferior lid margin. The procedure was first performed in the right eye and then repeated in the left eye with the same applicator. The cotton tip applicator was then broken and the tip placed in an Eppendorf tube and immediately placed in −80°C. Our meibum collection technique is unique. Most published collection methods used a metal

spatula.[11] We used cotton swabs that roll over the lid margin to collect meibum. We adopted this technique to minimize patient discomfort. However, our 'meibum samples' may consist not only of expressed meibum, but also of meibum plugs and other components including marginal epithelial cells, cellular debris, tears, and/or microbes.

Extraction and Analysis of Sphingolipids:

Sphingolipids were analyzed in the Lipidomics core at the Virginia Commonwealth University, Richmond, following previously published protocols.[28-33] Internal standards were purchased from Avanti Polar Lipids (Alabaster, AL). Internal standards were added to samples in 20 μL ethanol:methanol:water (7:2:1) as a cocktail of 500 pmol each. Standards for sphingoid bases and sphingoid base 1-phosphates were 17-carbon chain length analogs: C17-sphingosine, (2S,3R,4E)-2-aminoheptadec-4-ene-1,3-diol (d17:1-So); C17-sphinganine, (2S,3R)-2-aminoheptadecane-1,3-diol (d17:0-Sa); C17-sphingosine 1-phosphate, heptadecasphing-4-enine-1-phosphate (d17:1-So1P); and C17-sphinganine 1-phosphate, heptadecasphinganine-1-phosphate (d17:0-Sa1P). Standards for N-acyl sphingolipids were C12-fatty acid analogs: C12-Cer, N-(dodecanoyl)-sphing-4-enine (d18:1/C12:0); C12-Cer 1-phosphate, N-(dodecanoyl)-sphing-4-enine-1-phosphate (d18:1/C12:0-Cer1P); C12-sphingomyelin, N-(dodecanoyl)-sphing-4-enine-1-phosphocholine (d18:1/C12:0-SM); and C12-glucosylceramide, N-(dodecanoyl)-1-β-glucosyl-sphing-4-eine. The MS grade solvents (chloroform, # EM-CX1050; and methanol, # EM-MX0475, as well as formic acid (ACS grade, # EM-FX0440-7), were obtained from VWR (West Chester, PA).

For LC-MS/MS analyses, a Shimadzu LC-20 AD binary pump system coupled to a SIL-20AC autoinjector and DGU20A3 degasser coupled to an ABI 4000 quadrupole/linear ion trap (QTrap) (Applied Biosystems, Foster City, CA) operating in a triple quadrupole mode was used. Q1 and Q3 was set to pass molecularly distinctive precursor and product ions (or a scan across multiple m/z in Q1 or Q3), using N2 to collisionally induce dissociations in Q2 (which was offset from Q1 by 30-120 eV); the ion source temperature set to 500 °C.

Samples were collected into 13 × 100 mm borosilicate tubes with a Teflon-lined cap (catalog #60827-453, VWR, West Chester, PA). Then 1 mL of CH_3OH and 0.5 mL of $CHCl_3$ were added along with the internal standard cocktail (500 pmol of each species dissolved in a final total volume of 20 μl of ethanol:methanol:water 7:2:1). The contents were dispersed using an ultra sonicator at room temperature for 30 seconds. This single-phase mixture was incubated at 48°C overnight. After cooling, 75 μl of 1 M KOH in CH_3OH was added and, after brief sonication, incubated in a shaking water bath for 2 hours at 37°C to cleave potentially interfering glycerolipids. The extract was brought to neutral pH with 6 μl of glacial acetic acid, then the extract was centrifuged using a table-top centrifuge, and the supernatant was removed by a Pasteur pipette and transferred to a new tube. The extract was reduced to dryness using a Speed Vac. The dried residue was reconstituted in 0.5 mL of the starting mobile phase solvent for LC-MS/MS analysis, sonicated for 15 seconds, then centrifuged for 5 minutes in a tabletop centrifuge before transfer of the clear supernatant to the autoinjector vial for analysis. The sphingoid bases, sphingoid base 1-phosphates, and complex sphingolipids were separated by reverse phase LC using a Supelco 2.1 (i.d.) × 50

mm Ascentis Express C18 column (Sigma, St. Louis, MO) and a binary solvent system at a flow rate of 0.5 mL/min with a column oven set to 35°C. Prior to injection of the sample, the column was equilibrated for 30 seconds with a solvent mixture of 95% Mobile phase A1 ($CH_3OH/H_2O/HCOOH$, 58/41/1, v/v/v, with 5 mM ammonium formate) and 5% Mobile phase B1 ($CH_3OH/HCOOH$, 99/1, v/v, with 5 mM ammonium formate), and after sample injection (typically 40 μL), the A1/B1 ratio was maintained at 95/5 for 2.25 minutes, followed by a linear gradient to 100% B1 over 1.5 minutes, which was held at 100% B1 for 5.5 minutes, followed by a 0.5 minute gradient return to 95/5 A1/B1. The column was re-equilibrated with 95:5 A1/B1 for 30 seconds before the next run. The species of ceramide (Cer), hexosyl-ceramide (Hex-Cer), sphingomyelin (SM), sphingoid lipids such as sphingosine (Sph), dihydro-sphingosine (Dh-Sph), S1P, and Dh-S1P were identified based on their retention time and *m/z* ratio and quantified as described in previous publications.[29-31,33-38] The detailed MS parameters and species identification chart is shown in Supplemental Tables S1 and S2 and Supplemental Figures S1, S2, and S3.

Statistical Analysis:

Descriptive statistics were performed to summarize patient baseline demographics and clinical information. Associations between these predictor variables and various outcome variables including the amount of total and major sphingolipid species as well as sphingolipid composition, as determined by mole percent were assessed via parametric (independent samples T-test) or non-parametric (Spearman's rank order correlation and Mann-Whitney U) tests, as appropriate. Specifically, we employed non-parametric tests to compare the median and interquartile ranges of lipids in the MGD and control groups. Multiple linear regression analyses were carried out to assess the impact of demographic factors and clinical signs of MGD on our outcome variables. All statistical analyses were performed using SPSS 22.0 (SPSS, Inc., Chicago, IL).

RESULTS

Forty-three individuals participated in the study (mean age 55 ± 13.5 years; 77% men; 40% white, 54% black, 6% other; 26% Hispanic, 74% Non-Hispanic). While we graded three clinical parameters of MGD, we focused on meibum quality as our primary metric. After dividing individuals into two groups based on meibum quality, we found that individuals with poor meibum quality (n=21) were older (60 ± 8 years) than those with good quality (n=22) (51 ± 16 years) and more likely to be male (90% vs 64%) (Table 1).

We first quantified total SPL and major SPL classes (Cer, Hex-Cer, SM, S1P, and Sph) in meibum collected from all 43 patients (Table 2). SM and Hex-Cer are not thought to be bioactive, whereas the major bioactive sphingolipid species are Cer, Sph, and S1P. Cer and Sph are generally pro-apoptotic lipids, whereas S1P is an anti-apoptotic lipid (Figure 1).[22] We found that the IQR (25^{th} percentile - 75^{th} percentile) for total SPL (328.58 pmol), SM (200.13 pmol), Cer (174.98 pmol), Hex-Cer (28.90 pmol), Sph (5.13 pmol), and S1P (1.16 pmol) was fairly wide, reflecting the variance in amount of sample collected (Table 2).

We next compared amounts of SPL, Cer, Hex-Cer, SM, Sph, and S1P between the two groups. We found that individuals with poor meibum quality had lower levels (pmol) of SPL,

Cer, and Sph, significantly lower levels of Hex-Cer, and S1P and a higher level of SM (Table 3 and Figure 2A-F). Multiple linear regression models showed that age, race, gender, and ethnicity had no statistically significant impact on SPL, Cer, Hex-Cer, SM, Sph, or S1P levels.

Next, we compared the relative composition of SPL in the two groups.Comparing relative composition of the major SPL species via mole percent allowed for a normalized metric that was not dependent on the volume of meibum extracted. First, we found that as meibum quality worsened, the relative composition of Cer (rho= −0.38, p=0.013), Hex-Cer (rho= − 0.58, p<0.01), Sph (rho= −0.05, p=0.76), and S1P (rho= −0.29, p=0.06 decreased, and the relative composition of SM (rho= 0.41, p<0.01) increased. Next, we compared the mole percent of Cer, Hex-Cer, SM, Sph, and S1P. We found that individuals with poor meibum quality had SPL composed of less Cer (33.36% vs 49.49%, p<0.01), less Hex-Cer (4.88% vs 9.15%, p<0.01), less S1P (0.16% vs 0.31%, p=0.05) and more SM (58.67% vs 38.18%, p<0.01) and more Sph (2.92% vs 2.87%, p=0.97) as compared to individuals with good meibum quality (Table 4 and Figure 3A and 3B).

Each sphingolipid class is composed of lipids of different fatty acid chain lengths. In humans, six isoforms of ceramide synthase (CerS) have been identified and each produces a different subset of Cer, containing fatty acid chains of 14 to 32 carbons.[39] We investigated the mole percentages of major Cer species and found some significant differences between the two groups. Specifically, individuals with poor meibum quality had significantly higher median mole percentage of Cer C24:1 (p<0.01), Cer C24:0 (p<0.01), and Cer C26:0 (p=0.01); and significantly lower median mole percent of Cer C18:0 (p<0.01), Cer C20:0 (p<0.01), and Cer C22:0 (p<0.01) (Table 5 and Figure 4A).

We also compared mole percentages of major Hex-Cer and SM species between the groups and again found significant differences in a number of species between individuals with good versus poor quality meibum. Specifically, individuals with poor quality meibum had higher mole percentages of Hex-Cer C16:0 (p=0.01) and C26:0 (p=0.03) and lower mole percent of Hex-Cer C18:1 (p<0.01) and Hex-Cer C26:1 (p<0.01) (Figure 4B). Patients with poor meibum quality also had a significantly higher mole percent of SM C24:1 (p=0.013) and C26:1 (p=0.017) and a significantly lower mole percent SM C14:0 (p<0.01), SM C18:1 (p=0.01), and SM C18:0 (p<0.01) compared to those with good meibum quality. (Figure 4C).

Finally, we analyzed the ratio of mole percent of Cer to Hex-Cer, Cer to SM, and Cer to S1P. We found that in individuals with poor meibum quality, the Cer:Hex-Cer ratio (7.07 vs 5.57, p=0.03) and Cer:S1P (495.23 vs 282.69, p=0.07) increased, whereas the Cer:SM (1.19 vs 2.40, p=0.09) decreased (Table 4).

We then repeated our analysis examining our secondary predictor variables MG atrophy and MG plugging independent of meibum quality. Overall, we found similar results when examining these other facets of MGD. (Figure 2A-F and Figure 3C-F) Multiple linear regression models demonstrated that meibum quality was the only clinical sign of MGD that predicted relative composition (mole percent) of SM, Hex-Cer, and Cer (r^2 0.111-0.402,

p<0.05 for all). The models also showed that demographic factors did not influence mole percent of SM, Hex-Cer, Cer, Sph, or S1P.

DISCUSSION

In this study, we demonstrated that clinical signs of MGD correlated with compositional changes in commonly known sphingolipids in human meibum, which through structural and bioactive roles could potentially alter the composition of the TFLL and signal for apoptosis of MG cells. In assessing relative composition of meibum SPLs, we found that individuals with poor meibum quality had meibum that was composed of less Cer, less Hex-Cer, less S1P, more Sph, and more SM. We also found that longer-chain species of Cer, Hex-Cer and SM were increased in individuals with poor quality meibum versus those with good quality meibum. Finally, we analyzed the ratio of Cer and S1P composition, a ratio reflecting the relationship between pro-apoptotic (Cer) and anti-apoptotic (S1P) lipids, and found that the Cer to S1P ratio was increased in individuals with poor quality meibum versus those with good quality meibum.

SPL metabolism is complex and consists of many enzymes, alternate pathways, and feedback loops, with ceramides as a central hub (Figure 1).[22] Ceramides are produced through a *de novo* pathway or through the breakdown of SM by sphingomyelinases (SMases).[23,32] Once Cers are synthesized, there are several different possible fates. Cers can be converted to Sph and then S1P, to Hex-Cer, or back into SM (Figure 1).[22] The changes in relative SPL composition we observed may have both structural and functional effects.

Structurally, SPLs are part of the polar lipid monolayer that interfaces between the non-polar lipids and aqueous-mucin phase, and help maintain the integrity of the tear film.[16] Our findings of less Cer, Hex-Cer, S1P, and more Sph and SM in individuals with signs of MGD may point to TFLL destabilization as a result of alterations in the typical composition of these SPL metabolites. Interestingly, our findings have not been consistently reproduced in prior MGD studies where different percentages of SPL metabolites have been found in a variety of MGD models.[11,14,15,18,40]

In an *in vitro* study using meibum from healthy individuals, artificially increasing the percentage of Cer increased rigidity, melting temperature, and tear film disruption.[18] A similar detrimental effect of increased Cer percentage in meibum was demonstrated in a rabbit model of MGD. In this study, rabbits treated with epinephrine had a higher percentage of Cer in meibum as compared to untreated controls, which was associated with increased epidermal tissue in meibum, a sign of hyperkeratinization of the meibomian glands.[14] Yet, not all studies found an inverse relationship between Cer and stablity. In a computer simulation model, the presence of both SM and Cer in the polar lipid layer led to increased TFLL surface tension and enhanced structural stability.[41]

Human MGD is a more challenging disease to study given the disconnect between symptoms and signs of disease.[42] With this caveat, increases in relative composition of both SM and Cer were found in meibum of individuals with DE symptoms defined as Ocular Surface Disease Index (OSDI) score >21 as compared to individuals without symptoms

(OSDI <12.9).[40] In another study of individuals with chronic blepharitis and keratoconjunctivitis sicca (epithelial erosions, decreased tear meniscus), meibum was composed of less SM compared to controls.[11] Taken together, it is difficult to interpret the effect of Cer or SM in isolation, but these data indicate that there may be an optimal composition of these SPLs metabolites in meibum and that alterations in composition can lead to poor meibum quality.

Further information of the structural role of SPL can be gleaned by examining fatty acid chain lengths.[39,43-45] In humans, six isoforms of ceramide synthase (CerS1-CerS6) have been identified and each produces a different subset of Cer containing fatty acid chains of 14 to 32 carbons.[39] In general, sphingolipids in mammalian cells are mainly composed of saturated (eg. C16:0) and mono-unsaturated (C18:1) fatty acids.[46] The solublity of these lipids increases with an increase in unsaturation of the chain, whereas the solubility decreases as the fatty acid chains get longer, which may disrupt TFLL integrity. We found that individuals with clinical signs of MGD had increased relative composition of longer-chain lipids (24 and 26 carbon fatty acid chains), which are less soluble, and may contribute to tear film destabilization.

Regarding functional roles, SM and Hex-Cer are mainly found as cell membrane constituents and are not thought to be bioactive, whereas Cer, Sph, and S1P are bioactive SPLs and induce cellular signaling upon interaction with intracellular signaling proteins and cell surface receptors. The ratio of Cer and S1P composition is considered the most important metric when assessing the bioactive role of SPLs. The interconversion of Cer and S1P is known as the “sphingolipid rheostat” and shifts in the equilibrium of these two lipids in response to cellular stress favor either pro-apoptotic or anti-apoptotic signals from these bioactive sphingolipids.[47,48] Furthermore, because Cer and S1P are interconvertible, Kawabori et al[49] proposed that the composition of these lipids relative to each other, rather than their absolute amounts determine cell fate. We noted that while both Cer and S1P composition was lower in individuals with poor meibum quality, there was an increase in the Cer:S1P ratio in these individuals, possibly indicating a relative increase in pro-apoptotic lipids (Cer). It should be noted, however, that we only assessed lipid composition at one time point, so it is difficult to definitively make conclusions about directionality in the Cer and S1P equilibrium. Interestingly, many inflammatory mediators implicated in MGD[5,13] are also involved in SPL metabolism. The relationship is complex, where inflammatory mediators IL-1 and TNFα enhance both the breakdown of SM (non-bioactive) into Cer (pro-apoptotic) and the conversion of Sph (pro-apoptotic) into S1P (anti-apoptotic).[22]

Our study findings must be considered in light of its limitations. First, we used forceful expression to obtain our samples and therefore the extracted meibum may not be fully representative of the physiological meibum available to the ocular surface during normal blinking. Furthermore, some of our findings may be attributable to increased cellular rupture or presence of epithelial cells as a result of forceful expression. However, while we found increased SM, a common constituent of plasma membranes, in individuals with poor quality meibum, we concomitantly found a decreased Hex-Cer, another constituent of plasma membranes, in the same subset of individuals. Thus, attributing the noted changes to cellular rupture alone does not fully explain our findings. Additionally, our technique for collecting

meibum was designed to minimize discomfort, but may have allowed for mixing of our "meibum samples" with marginal epithelial cells and cellular debris, tears, and microbes. Other limitations of this study include a unique study population, a focus on specific clinical signs of MGD, and a lack of assessed inflammatory mediators.

In conclusion, we found an association between clinically observable signs of MGD and compositional changes in meibum SPLs. In short, we found an increase in the relative composition of SM and a concomitant decrease in Cer, along with an increase in longer-chain fatty acid species and an increase in the Cer to S1P ratio. We postulate that these changes may have both structural and functional implications. Further investigation of the structural and functional roles of SPLs in MGD is needed to improve our understanding of MGD pathophysiology, which may potentially aid in the development of therapeutics that target SPL pathways.

Supplementary Material

Refer to Web version on PubMed Central for supplementary material.

Acknowledgments

Funding statement: Supported by the Department of Veterans Affairs, Veterans Health Administration, Office of Research and Development, Clinical Sciences Research EPID-006-15S (Dr. Galor), R01EY026174 (Dr. Galor), R01EY022071 (Dr. Mandal), R21EY025256 (Dr. Mandal), RPB International Collaborators Award (Dr. Mandal), NIH Center Core Grant P30EY014801, P30EY021725 and Research to Prevent Blindness Unrestricted Grant.

Funding: Supported by the Department of Veterans Affairs, Veterans Health Administration, Office of Research and Development, Clinical Sciences Research EPID-006-15S (Dr. Galor), R01EY026174 (Dr. Galor), R01EY022071 (Dr. Mandal), R21EY025256 (Dr. Mandal), RPB International Collaborators Award (Dr. Mandal), NIH Center Core Grant P30EY014801, P30EY021725 and Research to Prevent Blindness Unrestricted Grant.

REFERENCES

1. Craig JP, Nelson JD, Azar DT, et al. TFOS DEWS II Report Executive Summary. Ocul Surf. 2017;15(4):802–812. [PubMed: 28797892]
2. Craig JP, Nichols KK, Akpek EK, et al. TFOS DEWS II Definition and Classification Report. Ocul Surf. 2017;15(3):276–283. [PubMed: 28736335]
3. Stapleton F, Alves M, Bunya VY, et al. TFOS DEWS II Epidemiology Report. The ocular surface. 2017; 15(3):334–365. [PubMed: 28736337]
4. Bron AJ, de Paiva CS, Chauhan SK, et al. TFOS DEWS II pathophysiology report. The ocular surface. 2017;15(3):438–510. [PubMed: 28736340]
5. Baudouin C, Messmer EM, Aragona P, et al. Revisiting the vicious circle of dry eye disease: a focus on the pathophysiology of meibomian gland dysfunction.The British journal of ophthalmology. 2016;100(3):300–306. [PubMed: 26781133]
6. McCulley JP, Shine WE. Meibomian gland function and the tear lipid layer. The ocular surface. 2003;1(3):97–106. [PubMed: 17075642]
7. Mathers WD. Ocular evaporation in meibomian gland dysfunction and dry eye. Ophthalmology. 1993;100(3):347–351. [PubMed: 8460004]
8. Jester JV, Nicolaides N, Kiss-Palvolgyi I, Smith RE. Meibomian gland dysfunction. II. The role of keratinization in a rabbit model of MGD. Investigative ophthalmology & visual science. 1989;30(5): 936–945. [PubMed: 2470694]
9. Hwang HS, Parfitt GJ, Brown DJ, Jester JV. Meibocyte differentiation and renewal: Insights into novel mechanisms of meibomian gland dysfunction (MGD). Experimental eye research. 2017.

10. Jester JV, Potma E, Brown DJ. PPARgamma Regulates Mouse Meibocyte Differentiation and Lipid Synthesis. The ocular surface. 2016;14(4):484–494. [PubMed: 27531629]
11. Shine WE, McCulley JP. Keratoconjunctivitis sicca associated with meibomian secretion polar lipid abnormality. Archives of ophthalmology (Chicago, III: 1960). 1998;116(7):849–852.
12. Shine WE, McCulley JP. Polar lipids in human meibomian gland secretions. Current eye research. 2003;26(2):89–94. [PubMed: 12815527]
13. Chhadva P, Goldhardt R, Galor A. Meibomian Gland Disease: The Role of Gland Dysfunction in Dry Eye Disease. Ophthalmology. 2017;124(11S):S20–S26. [PubMed: 29055358]
14. Nicolaides N, Santos EC, Smith RE, Jester JV. Meibomian gland dysfunction. III. Meibomian gland lipids. Investigative ophthalmology & visual science.1989;30(5):946–951. [PubMed: 2498228]
15. Robciuc A, Hyotylainen T, Jauhiainen M, Holopainen JM. Ceramides in the pathophysiology of the anterior segment of the eye. Current eye research. 2013;38(10):1006–1016. [PubMed: 23885886]
16. McCulley JP, Shine W. A compositional based model for the tear film lipid layer. Trans Am Ophthalmol Soc. 1997;95:79–88; discussion 88–93. [PubMed: 9440164]
17. Greiner JV, Glonek T, Korb DR, Booth R, Leahy CD. Phospholipids in meibomian gland secretion. Ophthalmic Res. 1996;28(1):44–49.
18. Arciniega JC, Uchiyama E, Butovich IA. Disruption and destabilization of meibomian lipid films caused by increasing amounts of ceramides and cholesterol. Investigative ophthalmology & visual science. 2013;54(2):1352–1360. [PubMed: 23341008]
19. Shine WE, McCulley JP. Meibomianitis: polar lipid abnormalities. Cornea. 2004;23(8):781–783. [PubMed: 15502478]
20. Gangoiti P, Camacho L, Arana L, et al. Control of metabolism and signaling of simple bioactive sphingolipids: Implications in disease. Prog Lipid Res. 2010;49(4):316–334. [PubMed: 20193711]
21. Bartke N, Hannun YA. Bioactive sphingolipids: metabolism and function. J Lipid Res. 2009;50 Suppl:S91–96. [PubMed: 19017611]
22. Hannun YA, Obeid LM. Principles of bioactive lipid signalling: lessons from sphingolipids. Nat Rev Mol Cell Biol. 2008;9(2):139–150. [PubMed: 18216770]
23. Chen H, Chan AY, Stone DU, Mandal NA. Beyond the cherry-red spot: Ocular manifestations of sphingolipid-mediated neurodegenerative and inflammatory disorders. Surv Ophthalmol. 2014;59(1):64–76. [PubMed: 24011710]
24. Galor A, Feuer W, Lee DJ, Florez H, Venincasa VD, Perez VL. Ocular surface parameters in older male veterans. Invest Ophthalmol Vis Sci. 2013;54(2):1426–1433. [PubMed: 23385801]
25. Arita R, Minoura I, Morishige N, et al. Development of Definitive and Reliable Grading Scales for Meibomian Gland Dysfunction. Am J Ophthalmol. 2016;169:125–137. [PubMed: 27345733]
26. Pult H, Nichols JJ. A review of meibography. Optom Vis Sci. 2012;89(5):E760–769. [PubMed: 22488268]
27. Bron AJ, Benjamin L, Snibson GR. Meibomian gland disease. Classification and grading of lid changes. Eye (London, England). 1991;5 (Pt 4):395–411.
28. Simanshu DK, Kamlekar RK, Wijesinghe DS, et al. Non-vesicular trafficking by a ceramide-1-phosphate transfer protein regulates eicosanoids Nature.2013;500(7463):463–467. [PubMed: 23863933]
29. Stiles M, Qi H, Sun E, et al. Sphingolipid profile alters in retinal dystrophic P23H-1 rats and systemic FTY720 can delay retinal degeneration. J Lipid Res. 2016;57(5):818–831. [PubMed: 26947037]
30. Wijesinghe DS, Allegood JC, Gentile LB, Fox TE, Kester M, Chalfant CE. Use of high performance liquid chromatography-electrospray ionization-tandem mass spectrometry for the analysis of ceramide-1-phosphate levels. J Lipid Res. 2010;51(3):641–651. [PubMed: 19654423]
31. Wijesinghe DS, Brentnall M, Mietla JA, et al. Ceramide kinase is required for a normal eicosanoid response and the subsequent orderly migration of fibroblasts. J Lipid Res. 2014;55(7): 1298–1309. [PubMed: 24823941]

32. Chen H, Tran JT, Eckerd A, et al. Inhibition of de novo ceramide biosynthesis by FTY720 protects rat retina from light-induced degeneration. J Lipid Res.2013;54(6): 1616–1629. [PubMed: 23468130]
33. Qi H, Priyadarsini S, Nicholas SE, et al. Analysis of sphingolipids in human corneal fibroblasts from normal and keratoconus patients. J Lipid Res. 2017;58(4):636–648. [PubMed: 28188148]
34. Shaner RL, Allegood JC, Park H, et al. Quantitative analysis of sphingolipids for lipidomics using triple quadrupole and quadrupole linear ion trap mass spectrometers. J Lipid Res. 2009;50(8): 1692–1707. [PubMed: 19036716]
35. Sullards MC, Allegood JC, Kelly S, et al. Structure-specific, quantitative methods for analysis of sphingolipids by liquid chromatography-tandem mass spectrometry: "inside-out" sphingolipidomics. Methods Enzymol. 2007;432:83–115. [PubMed: 17954214]
36. Hait NC, Allegood J, Maceyka M, et al. Regulation of histone acetylation in the nucleus by sphingosine-1-phosphate. Science. 2009;325(5945):1254–1257. [PubMed: 19729656]
37. Hait NC, Wise LE, Allegood JC, et al. Active, phosphorylated fingolimod inhibits histone deacetylases and facilitates fear extinction memory. Nat Neurosci. 2014;17(7):971–980. [PubMed: 24859201]
38. Alvarez SE, Harikumar KB Hait NC, et al. Sphingosine-1-phosphate is a missing cofactor for the E3 ubiquitin ligase TRAF2. Nature. 2010;465(7301):1084–1088. [PubMed: 20577214]
39. Grosch S, Schiffmann S, Geisslinger G. Chain length-specific properties of ceramides. Prog Lipid Res. 2012;51(1):50–62. [PubMed: 22133871]
40. Lam SM, Tong L, Yong SS, et al. Meibum lipid composition in Asians with dry eye disease. PloS one. 2011;6(10):e24339. [PubMed: 22043274]
41. Olzynska A, Cwiklik L. Behavior of sphingomyelin and ceramide in a tear film lipid layer model. Ann Anat. 2017;210:128–134. [PubMed: 27837653]
42. Nichols KK, Nichols JJ, MPH M, Mitchell GL. The Lack of Association Between Signs and Symptoms in Patients With Dry Eye Disease. Cornea. 2004;23(8):762–770. [PubMed: 15502475]
43. Hartmann D, Lucks J, Fuchs S, et al. Long chain ceramides and very long chain ceramides have opposite effects on human breast and colon cancer cell growth. Int J Biochem Cell Biol. 2012;44(4):620–628. [PubMed: 22230369]
44. Stiban J, Perera M. Very long chain ceramides interfere with C16-ceramide-induced channel formation: A plausible mechanism for regulating the initiation of intrinsic apoptosis. Biochim Biophys Acta. 2015;1848(2):561–567. [PubMed: 25462172]
45. Sassa T, Suto S, Okayasu Y, Kihara A. A shift in sphingolipid composition from C24 to C16 increases susceptibility to apoptosis in HeLa cells. Biochim Biophys Acta. 2012;1821(7):1031–1037. [PubMed: 22579584]
46. Brush RS, Tran JT, Henry KR, McClellan ME, Elliott MH, Mandal MN. Retinal sphingolipids and their very-long-chain fatty acid-containing species.Investigative ophthalmology & visual science. 2010;51(9):4422–4431. [PubMed: 20393115]
47. Van Brocklyn Williams JB Jr. The control of the balance between ceramide and sphingosine-1-phosphate by sphingosine kinase: oxidative stress and the seesaw of cell survival and death. Comparative biochemistry and physiology Part B, Biochemistry & molecular biology. 2012;163(1):26–36.
48. Hait NC, Oskeritzian CA, Paugh SW, Milstien S, Spiegel S. Sphingosine kinases, sphingosine 1-phosphate, apoptosis and diseases. Biochimica et Biophysica Acta (BBA) - Biomembranes. 2006;1758(12):2016–2026. [PubMed: 16996023]
49. Kawabori M, Kacimi R, Karliner JS, Yenari MA. Sphingolipids in cardiovascular and cerebrovascular systems: Pathological implications and potential therapeutic targets. World J Cardiol. 2013;5(4):75–86. [PubMed: 23675553]

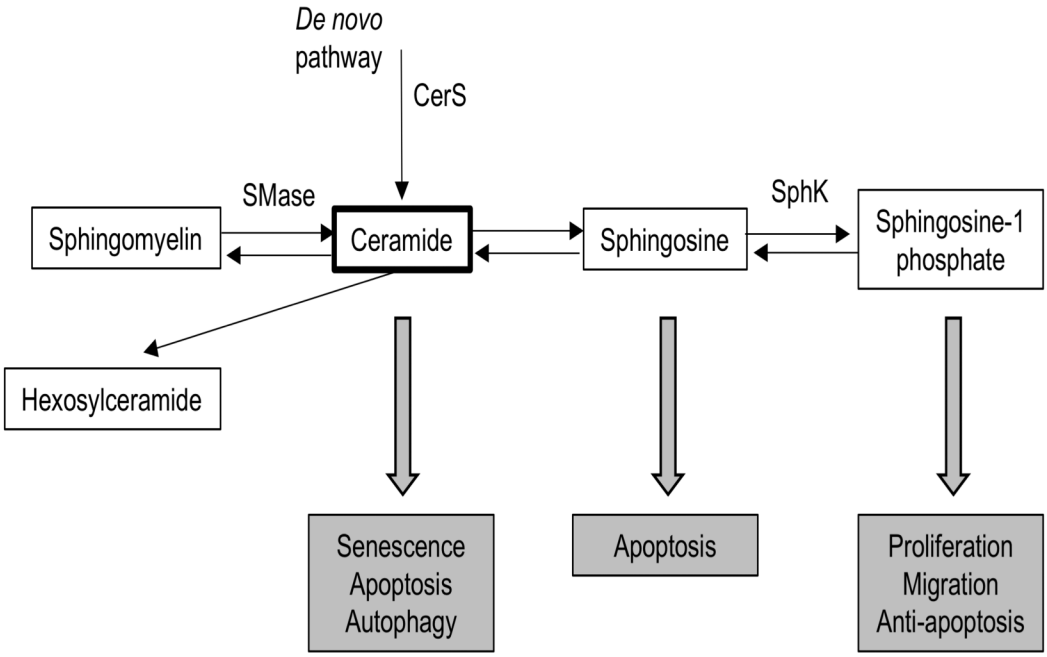

Figure 1:

Overview of sphingolipid metabolism and biological roles of bioactive sphingolipid species. Figure adapted from Hannun & Obeid (2008)[22]. Only enzymes thought to be potential therapeutic targets shown in this figure. Ceramide is synthesized through a *de novo* pathway catalyzed by serine palmitoyltransferase and ceramide synthase (CerS) or through the breakdown of sphingomyelin by sphingomyelinases (SMase). Sphingosine can be generated from ceramide by ceramidases and further converted into sphingosine 1-phosphate (S1P) by sphingosine kinase (SphK). Ceramide and sphingosine are overall pro-apoptotic lipids, whereas S1P has overall anti-apoptotic effects. Sphingomyelin and hexosylceramide are not known to be bioactive sphingolipids.

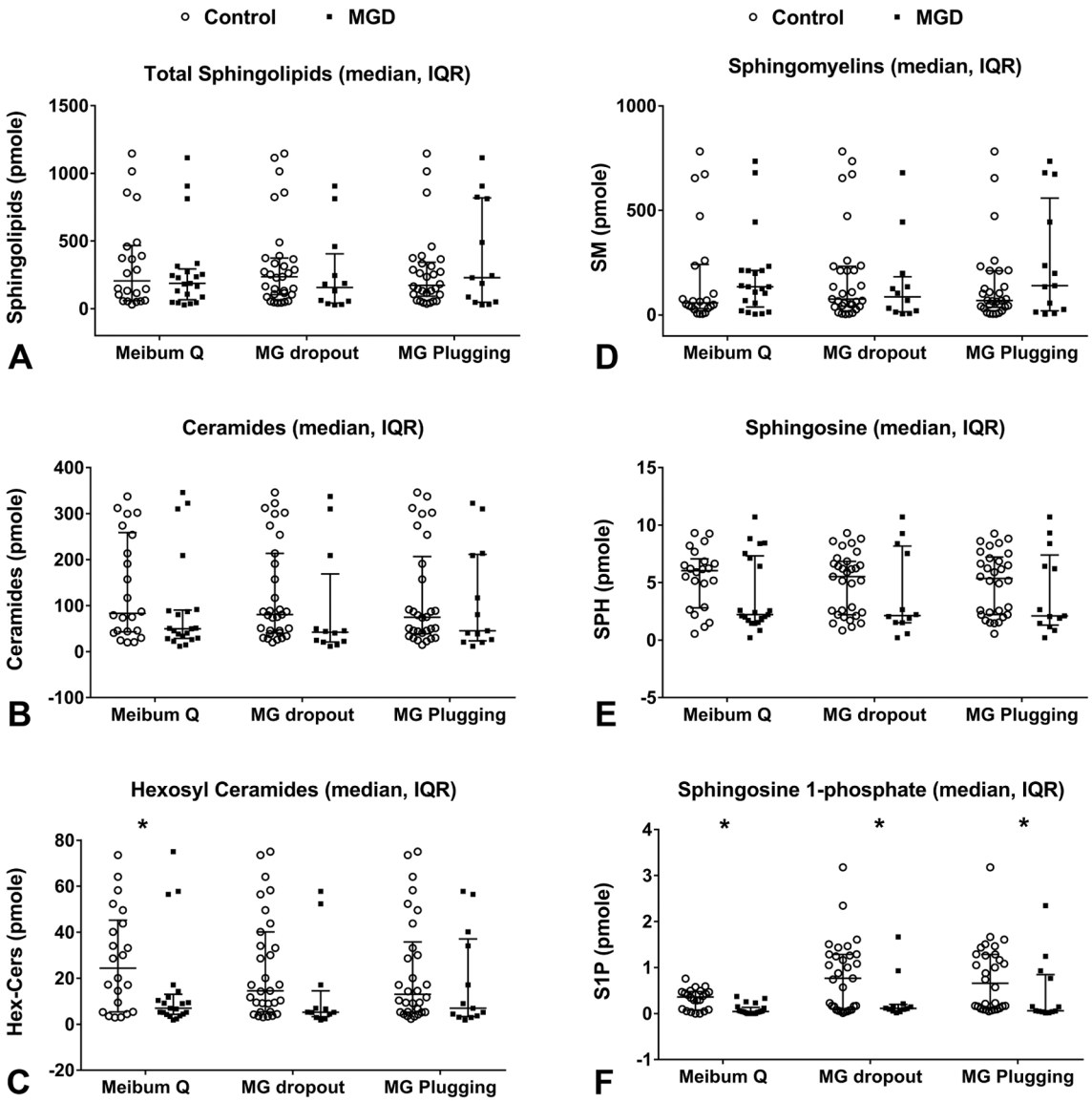

Figure 2:

LC-MS/MS analyses of human meibum conducted in triple quadrupole mode. Sphingoid bases, sphingosine 1-phosphate bases, and complex sphingolipids were separated by reverse phase LC using a C18 column, as described in the methods section. Amounts (pmol) of lipids were compared across groups defined by clinical parameters. Median amount and interquartile range are shown. **A.** Amount of total sphingolipids across clinical parameters. **B**. Amount of ceramide across clinical parameters **C.** Amount of hexosyl ceramide across clinical parameters. **D.** Amount of sphingomyelin across clinical parameters. **E**. Amount of sphingosine across clinical parameters. **F.** Amount of sphingosine 1-phosphate across clinical parameters. *Denotes statistical significance with p-value <0.05.

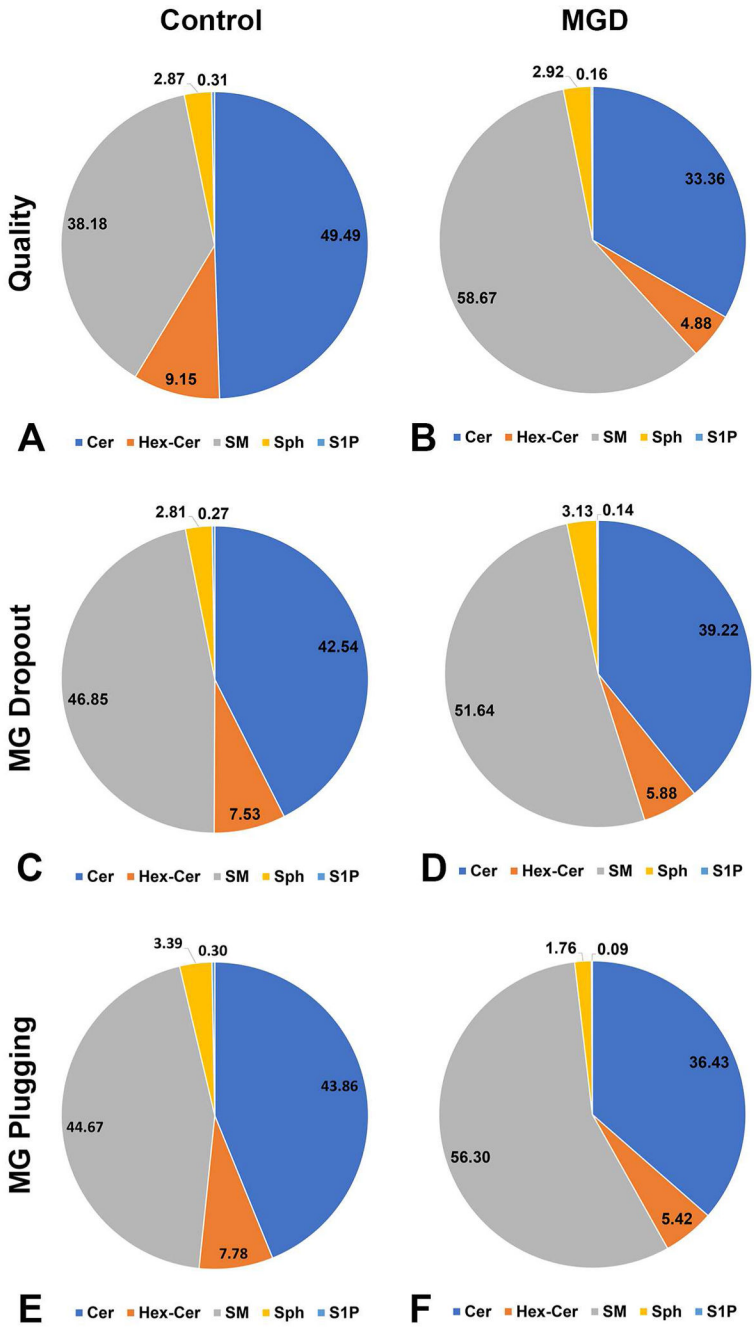

Figure 3.

LC-MS/MS analyses of human meibum conducted in triple quadrupole mode. Ceramide (Cer), hexosyl ceramide (Hex-Cer), and sphingomyelin (SM) were separated by reverse phase LC using a C18 column, as described in the methods section. The mole percent of Cer, Hex-Cer, and SM were compared across groups defined by clinical parameters. **A and B.** Comparison of mole percent of Cer, Hex-Cer, and SM with meibum quality. **C and D.** Comparison of mole percent of Cer, Hex-Cer, and SM with meibomian gland dropout. **E and F.** Comparison of mole percent of Cer, Hex-Cer, and SM with inferior meibomian gland plugging.

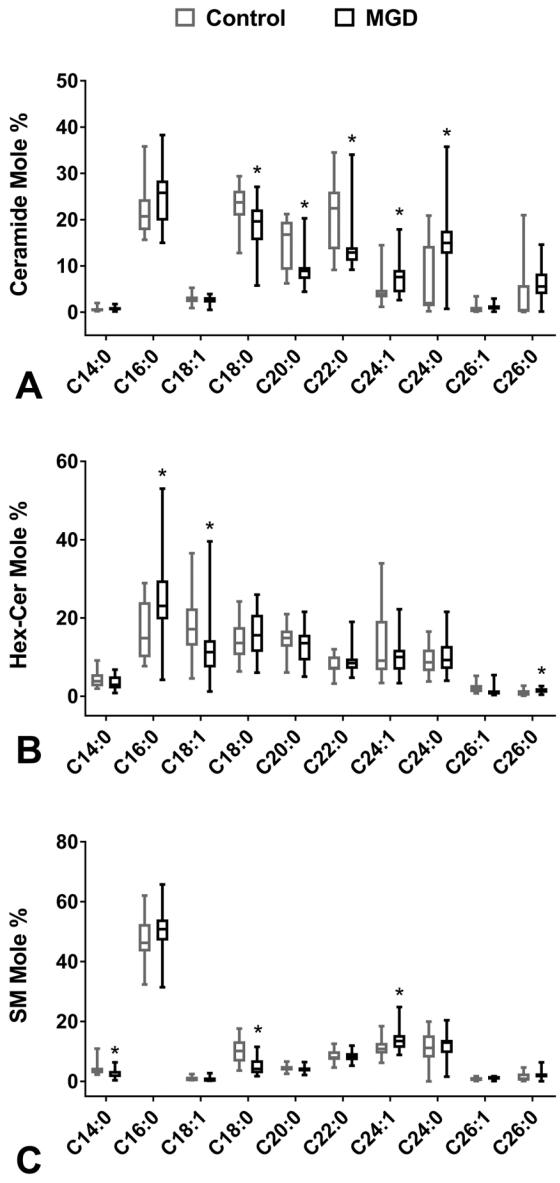

Figure 4.

LC-MS/MS analyses of human meibum conducted in triple quadrupole mode. The species of ceramide (Cer), hexosyl-ceramide (Hex-Cer), and sphingomyelin (SM) were identified based on their retention time and *m/z* ratio and quantified as described in previous publications.[30,31] The mole percent of species of Cer, Hex-Cer, and SM were compared across groups defined by clinical parameters. *Denotes statistical significance with p-value <0.05. Boxplots depicting the median, interquartile range, and range are shown. **A.** The mole percent of Cer species compared to meibum quality. **B.** The mole percent of Hex-Cer species compared to meibum quality. **C.** The mole percent of SM species compared to meibum quality.

Table 1.

Characteristics of groups based on meibum quality.

	Good Meibum Quality (N=22)	Poor Meibum Quality (N=21)	P-Value
Age (mean ± SD)	51 ± 16 years	60 ± 8 years	0.02
Sex (mean)	Male: 64% Female: 36%	Male: 90% Female: 10%	0.07
Race (mean)	White: 50% Black: 41% Other: 9%	White: 29% Black: 67% Other: 4%	0.32
Ethnicity (mean)	Hispanic: 27% Non-Hispanic: 73%	Hispanic: 24% Non-Hispanic: 76%	0.80

SD=standard deviation

Table 2.

Amount (pmol) of sphingolipid species.

Species Name	Median (N=43)	IQR
Cer	73.94	174.98
Hex-Cer	10.39	28.90
SM	76.48	200.13
Sph	5.16	5.13
S1P	0.21	1.16
SPL	187.00	328.58

SPL=total sphingolipid, Cer=ceramide, Hex-Cer=hexosyl ceramide, SM=sphingomyelin, Sph=sphingosine, S1P=sphingosine 1-phosphate, IQR=interquartile range

Table 3.

Amount (pmol) of major sphingolipid classes versus meibum quality.

Sphingolipid Species	Good Quality (N=22)		Poor Quality (N=21)		P-Value
	Median	IQR	Median	IQR	
SPL	205.75	406.8	187	257.58	0.61
Cer	83.22	215.71	49.7	61.31	0.2
Hex-Cer	24.4	39.85	6.98	8.67	0.03
SM	58.05	211.05	134.73	184.85	0.23
Sph	6.05	4.26	2.22	5.71	0.13
S1P	1.03	1.14	0.15	0.33	0.04

SPL=total sphingolipid, Cer=ceramide, Hex-Cer=hexosyl ceramide, SM=sphingomyelin, Sph=sphingosine, S1P=sphingosine 1-phosphate, IQR=interquartile range

Table 4.

Relative composition of major sphingolipid classes versus meibum quality.

Sphingolipid Species	Good Quality (N=22) Mole Percent		Poor Quality (N=21) Mole Percent		P-Value
	Mean	SE	Mean	SE	
Cer	49.49	19.25	33.36	16.98	<0.01
Hex-Cer	9.15	2.89	4.88	2.19	<0.01
SM	38.18	21.84	58.67	20.82	<0.01
Sph	2.87	2.26	2.92	4.37	0.97
S1P	0.31	0.23	0.16	0.25	0.05
Cer:Hex-Cer *	5.57	0.47	7.07	0.45	0.03
Cer:S1P *	282.69	67.43	495.23	93.08	0.07
Cer:SM *	2.40	0.51	1.19	0.47	0.09

Cer=ceramide, Hex-Cer=hexosyl ceramide, SM=sphingomyelin, Sph=sphingosine, S1P=sphingosine 1-phosphate, SE=standard error of the mean

* Ratios were first calculated for each individual and then mean ratios were compared between groups

Table 5.

Composition of major ceramide species versus meibum quality.

Fatty Acid Chain Length	Good Quality (N=22) Median Mole Percent (%)	Poor Quality (N=21) Median Mole Percent (%)	P-Value
Cer C14:0	0.48	0.74	0.13
Cer C16:0	20.70	25.79	0.06
Cer C18:1	2.57	2.65	0.63
Cer C18:0	23.74	19.63	<0.01
Cer C20:0	16.76	8.92	<0.01
Cer C22:0	22.44	12.89	<0.01
Cer C24:1	3.91	7.60	<0.01
Cer C24:0	1.94	14.96	<0.01
Cer C26:1	0.32	1.05	0.07
Cer C26:0	0.36	5.56	0.01

Cer=ceramide